

Measurement of charge-transfer-rate coefficients of ground-state He^+ with N_2 and CH_4 at electron-volt energies

Z. Fang, D. Chen, and Victor H. S. Kwong

Department of Physics, University of Nevada, Las Vegas, 4505 Maryland Parkway, Las Vegas, Nevada 89154

(Received 15 November 1999; revised manuscript received 12 June 2000; published 13 September 2000)

The rate coefficients for the dissociative charge-transfer reaction of $\text{He}^+ + \text{N}_2 \rightarrow \text{products}$ and $\text{He}^+ + \text{CH}_4 \rightarrow \text{products}$ are measured using ion storage. Helium ions were produced by electron bombardment of helium gas. The ion population in the trap was measured as a function of the storage time to give the reaction rate. The rate coefficient for He^+ and N_2 is $1.07(\pm 0.11) \times 10^{-9} \text{ cm}^3 \text{ s}^{-1}$, and the rate coefficient for He^+ and CH_4 is $1.73(\pm 0.29) \times 10^{-9} \text{ cm}^3 \text{ s}^{-1}$. The equivalent temperature for the two reactions was estimated to be 8700 and 8000 K, respectively. Our results are essentially the same as those obtained previously at 300 K.

PACS number(s): 34.70.+e, 82.30.Fi, 32.80.Pj, 95.30.Dr

I. INTRODUCTION

Rate coefficients and cross sections for ion-molecule reactions play an important role in the chemical models of earth's ionosphere, planetary atmosphere, dense molecular clouds, cometary comae, interstellar clouds, and supernova ejecta. Since the mid-1970's, laboratory research has produced a large body of such data for singly ionized elements such as He, N, O, and C reacting with molecules that include N_2 , O_2 , CH_4 , H_2O , CO, and CO_2 known to be present in various astrophysical regions. However, most of these measurements were made exclusively at temperatures between 298 and 700 K using drift tube techniques [1]. The limit on the temperature range was due to ions that came into thermal equilibrium with the carrier gas [1]. Furthermore, the temperatures of most of the planetary atmospheres and regions considered are low. Recent interest in the modeling of the chemical pathways in the hotter supernova ejecta and the x-ray emission mechanisms in comet atmospheres [2] required ion-molecule reaction data at a much higher temperature. As a case in point, with limited data at a much higher temperature, recent work by Lepp *et al.* [3] and Liu *et al.* [4] in the modeling of chemical pathways inside the supernova ejecta (SN1987A) had to use the dissociative charge-transfer rate coefficient for $\text{He}^+ + \text{CO} \rightarrow \text{products}$ at 300 K even though the temperature of the supernova ejecta is more than an order of magnitude higher. Despite the temperature independence of this reaction between 300 and 8700 K [5], there are cases where distinct temperature dependence has been observed, e.g., $\text{He}^+ + \text{NH}_4 \rightarrow \text{products}$ [6]. Calculation of the charge-transfer cross section between ion and molecule has been difficult due to the uncertainty of the potential curve of the pseudomolecule formed during collision. Therefore, it is essential that the experimental study of ion-molecule reactions be extended to and beyond the temperature of a few thousand degrees. In addition, these measurements can also serve to assess various assumptions made in the calculations.

Ion trap techniques have, in the last decade, demonstrated their suitability in measuring charge-transfer-rate coefficients at temperatures of a few thousand degrees [7,8]. In this paper we focus on two measurements, $\text{He}^+ + \text{N}_2 \rightarrow \text{products}$ and $\text{He}^+ + \text{CH}_4 \rightarrow \text{products}$, and report the measurement of the

total dissociative charge-transfer-rate coefficients for these two ion-molecule reactions at eV energies using an ion trap.

II. EXPERIMENTAL METHOD

The measurements of the rate coefficients of the reactions $\text{He}(1s) + \text{N}_2 \rightarrow \text{products}$ and $\text{He}(1s) + \text{CH}_4 \rightarrow \text{products}$ are carried out by using ion storage techniques. The facilities used in this experiment have been described in earlier publications [9]. A cylindrical quadrupole radio-frequency (rf) ion trap was used to store He^+ ions. Helium ions were created by the electron bombardment of helium. An unfocused electron beam was produced by a BaO dispenser cathode located outside one of the end cap electrodes of the ion trap. The dispenser cathode was biased at -150 V for 3 ms, thus producing and injecting a 3-ms-150 eV-pulsed electron beam into the ion trap. Immediately after this ion creation phase, the bias voltage was switched to $+100 \text{ V}$ to prevent further electron emission. The trapping parameters (rf frequency $f = 1.749 \text{ MHz}$, amplitude $V_0 = 295 \text{ V}$, and dc bias $U_0 = 22 \text{ V}$) of the rf quadrupole ion trap were chosen to selectively store He^+ ions. The estimated axial and radial pseudopotential well depth for He^+ were $D_z = 12.8 \text{ V}$ and $D_r = 14.2 \text{ V}$. The mean energy of the He^+ ions was estimated to be about 1.28 eV [10]. At these trapping parameters, ions produced by the electron bombardment of the target gas N_2 and CH_4 , i.e., $\text{N}_2^+(m/q=28)$, $\text{N}^+(m/q=14)$, $\text{C}^+(m/q=12)$, $\text{He}^{2+}(m/q=2)$, $\text{H}_2^+(m/q=2)$, and $\text{H}^+(m/q=1)$, were excluded from the trap. The operating points for $\text{C}^{2+}(m/q=6)$ and $\text{N}^{2+}(m/q=7)$ were near the edge of the stability region of the trap. These ions were not likely to be stored in the trap. By controlling the intensity and the energy of the electron beam, we found none of these ions in the trap. The mass spectrum shows He^+ ions were the only ions stored in the trap.

The rate coefficients of He^+ and N_2 , and He^+ and CH_4 reactions were determined by measuring the He^+ population in the trap as a function of time after they were created and stored in the trap in the presence of a target gas of known density. To measure the population of the stored He^+ , these ions were extracted from the trap by simultaneously biasing the upper and the lower end cap electrodes to $+100$ and

−150 V, respectively. These push-pull pulses emptied all the ions from the trap into a 0.3 m time-of-flight (TOF) mass spectrometer for ion identification. These ions were detected by a 1-in.-diam dual-microchannel-plate ion detector. The TOF mass spectrum was recorded by a Tektronix transient digitizer and stored in a computer for later analysis. The TOF spectrum served to identify the ion species, and its signal intensity was used to measure the ion population in the trap prior to the extraction.

To minimize the short-term and the long-term ion signal fluctuation and the drift due to the electron-beam intensity change, the ion signals were measured, alternately, at a delay time t after the ion production, and at the shortest delay time $t_0 = 25$ ms. The ion intensity ratio $I_r = I_t/I_{t_0}$ was then computed to obtain a relative intensity at time t . More than 100 pairs of such measurements were made. This gave the average value of the relative ion intensity and its statistical uncertainty at time t . The storage time was then scanned at a later time with a time increment δt to obtain the relative ion intensity vs time curve. Since the measurements were performed 25 ms after the ion was created, all He^+ ions were expected to be in their $1s$ ground state [11].

In each experiment, the decay rates of the stored He^+ ions were measured at several pressures of the target gas. The rate coefficient (k) of the reaction was derived from the slope of the target gas density-dependent decay rates:

$$\frac{1}{T} = \frac{1}{T_0} + kn, \quad (1)$$

where $1/T$ is the decay rate of the stored He^+ ions in the presence of the target gas of the density n , and $1/T_0$ is the He^+ ion loss rate without target gas admitted into the reaction chamber. This loss is caused by the charge-transfer interactions and the collision-induced rf heating (cf. Sec. III) of He^+ with the heavier residual gases in the chamber ($\leq 2.5 \times 10^{-10}$ Torr with H_2 , H_2O , and CO as main residual molecules), as well as the radiative association reaction of He^+ with helium (1.6×10^{-8} Torr) used to create He^+ .

In all the measurements, the ultrahigh-purity grade gases were used. These gases included He (99.999%), N_2 (99.999%), and CH_4 (99.99%). The helium gas and the target gas were introduced into the reaction chamber through separate gas handling systems. The leak valve between the reservoir and the vacuum chamber controlled the flow rate of the gas into the vacuum chamber, thus providing a fine control of the pressure of each gas for the experiment. The pressure of the gas was measured by a calibrated quadrupole residual gas analyzer. The calibration procedure was discussed in the previous publication [9]. The purity of the gases in the vacuum chamber was also confirmed by this quadrupole residual gas analyzer.

III. RESULTS AND DISCUSSION

Figures 1 and 2 show the relative intensities of He^+ as a function of storage time for N_2 and CH_4 , respectively, at several gas pressures. The solid lines represent the least-square fits of the data to a single-exponential function. The

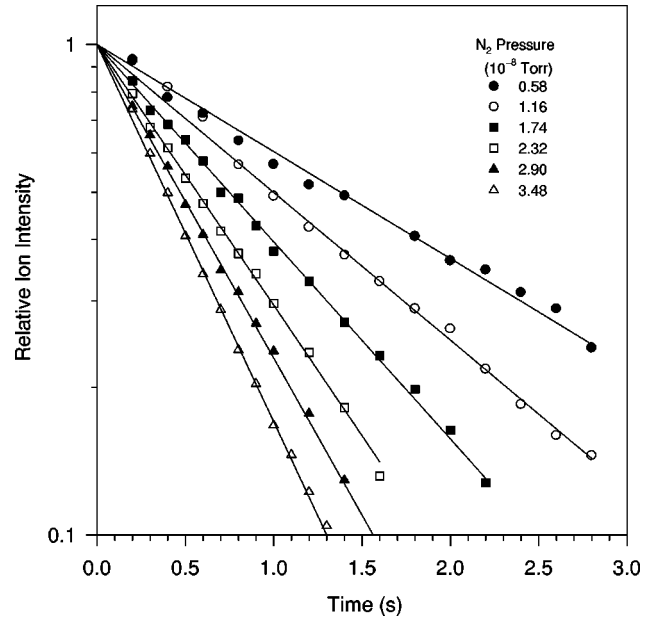


FIG. 1. The decay curves of normalized relative intensity of He^+ ion vs storage time at five different pressures of N_2 . Each data point represents more than 100 measurements. Solid lines are the least-squares fit to a single exponential function.

monotonous increase in the reaction rate with increasing target gas pressure is shown in Figs. 3 and 4. The slopes of the curves are obtained by a weighted least-squares fit to a linear function according to Eq. (1). The rate coefficients derived from the slopes are $1.38(0.10) \times 10^{-9} \text{ cm}^3 \text{ s}^{-1}$ for $\text{He}^+ + \text{N}_2 \rightarrow \text{products}$ and $2.12(0.23) \times 10^{-9} \text{ cm}^3 \text{ s}^{-1}$ for $\text{He}^+ + \text{CH}_4 \rightarrow \text{products}$. The estimated uncertainties of the results are mainly due to the uncertainty on the statistical fluctuation of the ion signals (typically about $\pm 4\%$) and the uncertainty

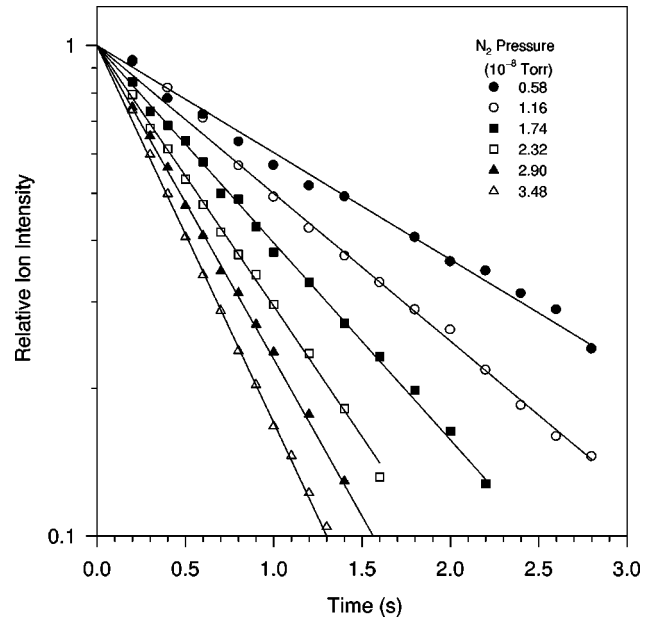


FIG. 2. The decay curves of the normalized relative intensity of He^+ ion vs storage time at five different pressures of CH_4 .

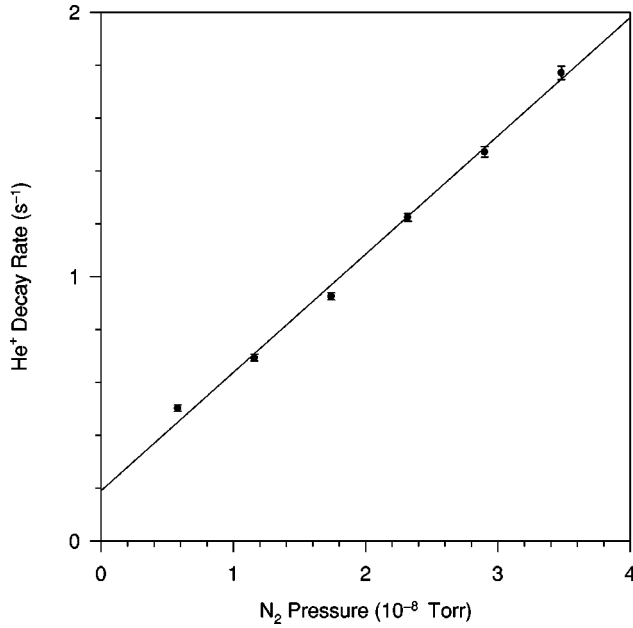


FIG. 3. He^+ ion decay rate vs N_2 pressure. Each error bar represents the statistical uncertainty of 1σ . The slope of the straight-line fit gives the charge-transfer-rate coefficient of the He^+ ion with N_2 .

on the estimation of the target gas density ($\pm 6\%$ for N_2 and $\pm 10\%$ for CH_4).

Since He^+ ions are much lighter than the target molecules, elastic collision in an rf field can induce heating of the stored He^+ ions. If the collision happens near the edge of the trap, this rf heating will likely cause the He^+ ions to leave the trap. This loss rate is a function of energy gained

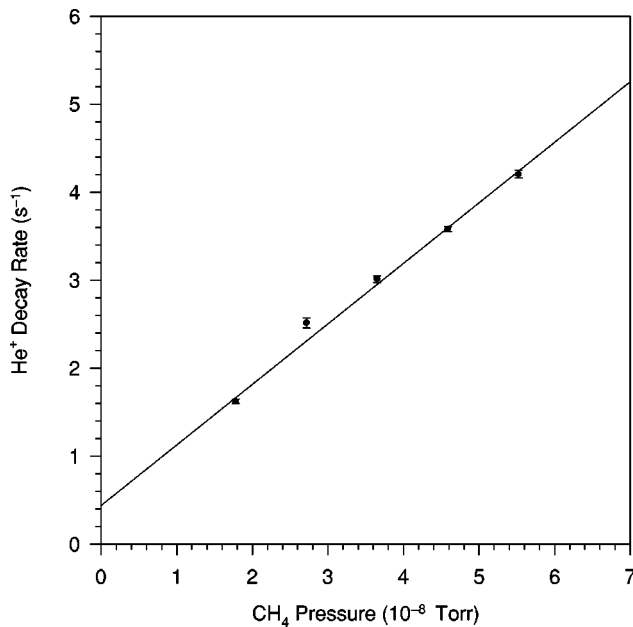


FIG. 4. He^+ ion decay rate vs CH_4 pressure. Each error bar represents the statistical uncertainty of 1σ . The slope of the straight-line fit gives the charge-transfer-rate coefficient of the He^+ ion with CH_4 .

by He^+ in the collision and the size of the elastic collision cross section. This ion loss will contribute a systematic error to the rate coefficient measurement. A binary collision model on the energy change in an elastic collision between an ion and a neutral particle in an rf field is given in the Appendix.

In the following paragraphs, the results developed in the Appendix will be used to estimate the mean energy change of a stored ion of mass m and charge q in a collision with a neutral particle of mass m_n in a rf field $\mathbf{E}(\mathbf{x}) = \mathbf{E}_0(\mathbf{x}) \sin \omega t$. The method of estimation of the correction factors for the rf heating ion loss will also be discussed.

In an rf ion trap, when an ion undergoes an elastic collision with a heavier neutral particle, the ion will, in average, gain kinetic energy through the collision, despite that the neutral particle is much cooler than the ion, because the rf heating overwhelms the collisional cooling [see Eqs. (A28) and (A29) in the Appendix]. When the collision occurs near the trap electrodes, the heating effect is the strongest. Using Eq. (A25) in the Appendix, the cycle average for the mean energy change of an ion in a collision with a neutral particle in an arbitrary direction is given by

$$\langle \Delta \bar{K} \rangle = \frac{2m_n^2}{(m+m_n)^2} \frac{q^2 E_0^2}{4m\omega^2} - \frac{2mm_n}{(m+m_n)^2} \left(\frac{1}{2} m u^2 - \frac{1}{2} m_n v_n^2 \right), \quad (2)$$

where u is the ion's drift velocity for the secular motion before the collision, and v_n is the velocity of the neutral particle before the collision. For an ion near the trap electrodes, where the rf field is the largest, the dominant motion is rf oscillation, with the drift velocity $u \approx 0$, therefore

$$\frac{q^2 E_0^2}{4m\omega^2} \approx \bar{W}, \quad (3)$$

where \bar{W} is the total kinetic energy of the ion averaged over a rf period, and is a constant of the secular motion [see Eqs. (A3), (A6), and (A7)]. If the neutral particle is at room temperature, we can ignore the term $\frac{1}{2} m_n v_n^2$. The change in the kinetic energy of the ion is

$$\langle \Delta \bar{K} \rangle = \frac{2m_n^2}{(m+m_n)^2} \bar{W}. \quad (4)$$

Because of the mass difference between He^+ and N_2 , and He^+ and CH_4 , the lighter He^+ ion gains a substantial amount of energy during this elastic collision. The mean kinetic-energy gain for the collision near the electrode between He^+ and N_2 , and between He^+ and CH_4 , is $1.55\bar{W}$ and $1.3\bar{W}$, respectively. In a near head-on collision, the maximum energy gain by He^+ is twice of the mean. Depending on the energy and position of the ion during collision, the extra energy can eject the ions from the trap near its edge. This ion loss needs to be estimated experimentally.

We chose Ar and Ne to estimate the ion loss for N_2 and CH_4 because of their similar mass ratios between the target molecule and He^+ , i.e., $m_{\text{N}_2}/m_{\text{He}} = 7$ and $m_{\text{Ar}}/m_{\text{He}} = 10$, and $m_{\text{CH}_4}/m_{\text{He}} = 4$ and $m_{\text{Ne}}/m_{\text{He}} = 5$. Furthermore, both Ar and

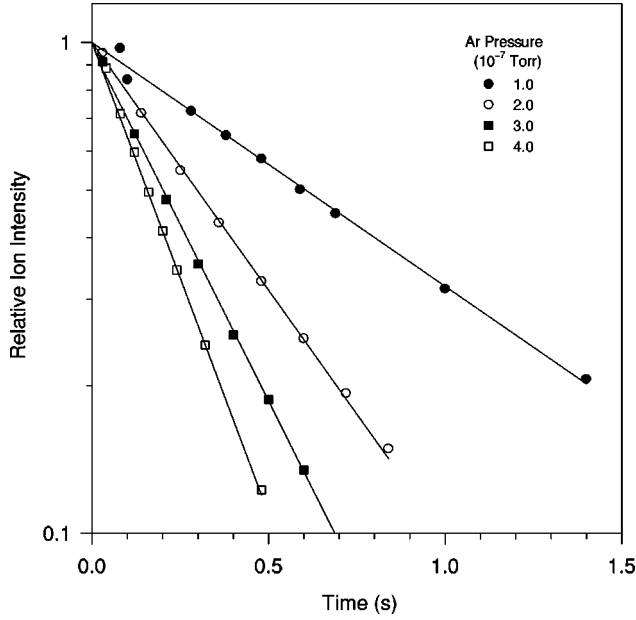


FIG. 5. The decay curves of the normalized relative intensity of He^+ ion vs storage time at four different pressures of Ar.

Ne are relatively inert to He^+ ions. We carried out the measurement of the ion loss rate coefficients of He^+ in the trap with Ar and Ne at the same trapping parameters used in the current measurements for N_2 and CH_4 . Figure 5 shows the decay curves of the He^+ at four different pressures of Ar and the least-squares fit to a single exponential function. Our measured He^+ loss rate coefficients are $0.31(0.03) \times 10^{-9} \text{ cm}^3 \text{ s}^{-1}$ in the presence of Ar and $0.22(0.03) \times 10^{-9} \text{ cm}^3 \text{ s}^{-1}$ in the presence of Ne. Since the maximum charge-transfer-rate coefficients are less than $10^{-11} \text{ cm}^3 \text{ s}^{-1}$ for Ar and less than $10^{-13} \text{ cm}^3 \text{ s}^{-1}$ for Ne [1], these ion loss rate coefficients must be caused by the collision-induced rf driven ion loss. These loss rates, however, may not be applied directly as correction factors in the current measurements since the elastic collision cross sections are different for different atoms and molecules. These coefficients need to be adjusted to reflect the differences in the elastic collision cross sections between Ar and N_2 , and Ne and CH_4 .

Elastic collision between ion and neutral molecules is primarily Coulombic. The cross section σ_e is directly related to the molecule's polarizability α with $\sigma_e \propto \alpha^{1/2}$. Since N_2 molecules have a similar polarizability ($\alpha = 1.73 \times 10^{-24} \text{ cm}^3$) to that of Ar ($\alpha = 1.64 \times 10^{-24} \text{ cm}^3$), it was estimated that the collision-induced rf driven ion loss for the He^+ and N_2 reaction is about $0.31 \times 10^{-9} \text{ cm}^3 \text{ s}^{-1}$ with 12% uncertainty. On the other hand, CH_4 has a larger polarizability ($\alpha = 2.6 \times 10^{-24} \text{ cm}^3$) than that of Ne ($\alpha = 0.40 \times 10^{-24} \text{ cm}^3$). Therefore, the elastic collision cross section of He^+ with CH_4 can be 2.6 times larger than that of He^+ with Ne. It was estimated that the collision-induced rf driven ion loss for the He^+ and CH_4 reaction is between 0.22 and $0.56 \times 10^{-9} \text{ cm}^3 \text{ s}^{-1}$, or $0.39(\pm 0.17) \times 10^{-9} \text{ cm}^3 \text{ s}^{-1}$. The corrected rate coefficient for the dissociative charge-transfer reaction of $\text{He}^+ + \text{N}_2 \rightarrow \text{products}$ is $1.07(\pm 0.11) \times 10^{-9} \text{ cm}^3 \text{ s}^{-1}$, and the rate coefficient for $\text{He}^+ + \text{CH}_4 \rightarrow$

products is $1.73(\pm 0.29) \times 10^{-9} \text{ cm}^3 \text{ s}^{-1}$.

Since the target molecules N_2 and CH_4 are at room temperature (300 K) and the stored He^+ ions have an average kinetic energy of 1.28 eV, which corresponds to a temperature of $9.9 \times 10^3 \text{ K}$, an equivalent temperature T_{equiv} is introduced to reflect the mean relative velocity of the He^+ and the target molecules [12]. The estimated T_{equiv} for the He^+ and N_2 reaction is 8700 K, and that for He^+ and CH_4 is 8000 K.

Significant amounts of work using the drift tube and its variations have been accumulated for both reactions [1]. Most of the measurements were carried out at room temperature. The mean values for the dissociative charge-transfer-rate coefficients measured at 300 K for He^+ and N_2 and for He^+ and CH_4 are $1.31(\pm 0.21) \times 10^{-9} \text{ cm}^3 \text{ s}^{-1}$ and $1.44(\pm 0.19) \times 10^{-9} \text{ cm}^3 \text{ s}^{-1}$, respectively. These values are essentially the same, within experimental uncertainties, as those reported here at a much higher temperature. It is reasonable, then, to assume that the coefficients for these reactions are not temperature dependent within this temperature range.

ACKNOWLEDGMENTS

The authors thank Hui Gao and Stephen Lepp for their helpful discussions. We also acknowledge the technical assistance of Bill O'Donnell. This work is supported by NASA under Grant No. NAG5-6727 to UNLV.

APPENDIX

In a quadrupole rf ion trap, an ion of mass m and charge q is subjected to the electric field

$$\mathbf{E}(\mathbf{x}, t) = \mathbf{E}_0(\mathbf{x}) \sin \omega t. \quad (\text{A1})$$

If the frequency ω is sufficiently high, the motion of the ion can be considered as the combination of a sinusoidal oscillation with frequency ω and a slowly varying (in terms of $1/\omega$) secular motion [13,14]. For the rf oscillation, the electric field can be treated to be quasi-uniform under the condition

$$\left| \frac{d\mathbf{E}_0(\mathbf{x})}{d\mathbf{x}} \cdot \mathbf{r}_0 \right| \ll |\mathbf{E}_0(\mathbf{x})|, \quad (\text{A2})$$

where \mathbf{r}_0 is the displacement of the ion within a period of the oscillation. The slowly varying secular motion is governed by the electric pseudopotential,

$$\psi(\mathbf{x}) = \frac{q|\mathbf{E}_0(\mathbf{x})|^2}{4m\omega^2}. \quad (\text{A3})$$

The velocity solution for Eq. (A1) therefore is

$$\mathbf{v} = -\frac{q\mathbf{E}_0}{m\omega} \cos \omega t + \mathbf{u}, \quad (\text{A4})$$

where \mathbf{u} represents the secular motion with

$$\left| \frac{2\pi \dot{\mathbf{u}}}{\omega} \right| \ll |\mathbf{u}|. \quad (\text{A5})$$

[For simplicity, we use \mathbf{E}_0 instead of $\mathbf{E}_0(\mathbf{x})$ in Eq. (A4) and later on.] The time average kinetic energy of the ion for one rf period is

$$\bar{K} = \frac{q^2 |\mathbf{E}_0|^2}{4m\omega^2} + \frac{1}{2}m|\mathbf{u}|^2, \quad (\text{A6})$$

or, by using Eq. (A3),

$$\bar{K} = q\psi + K_s = \bar{W}, \quad (\text{A7})$$

where K_s is the kinetic energy of the secular motion, and \bar{W} is the total kinetic energy averaged over one period. \bar{W} is a constant for the secular motion. By averaging over the secular motion period, we also have

$$q\bar{\psi} = \frac{1}{2}\bar{W}, \quad (\text{A8})$$

$$\bar{K}_s = \frac{1}{2} \bar{W}. \quad (\text{A9})$$

Consider an ion in a binary collision with another particle. The velocity of the ion after the collision is

$$v' = -\frac{q\mathbf{E}_0}{m\omega}\cos\omega t + \mathbf{u} + \Delta\mathbf{v}, \quad (\text{A10})$$

where $\Delta \mathbf{v}$ is the instantaneous velocity change due to the collision. The kinetic-energy change averaged over one rf period is

$$\Delta \bar{K} = \frac{1}{2} m (|\Delta \mathbf{v} + \mathbf{u}|^2 - |\mathbf{u}|^2) \quad (\text{A11})$$

$$= \frac{1}{2}m(|\Delta \mathbf{v}|^2 + 2\Delta \mathbf{v} \cdot \mathbf{u}). \quad (\text{A12})$$

In the following, this energy change will be explicitly evaluated.

Suppose that an ion collides with a neutral atom/molecule of mass m_n at time t_0 ; the ion's velocity prior to the collision is given by Eq. (A4),

$$\mathbf{v}_i = -\frac{q\mathbf{E}_0}{m\omega} \cos \omega t_0 + \mathbf{u}; \quad (\text{A13})$$

and the atom/molecule's velocity prior to the collision is \mathbf{v}_n . The velocity of the center-of-mass (c.m.) of the ion-neutral pair is

$$\mathbf{v}_c = \frac{m\mathbf{v}_i + m_n\mathbf{v}_n}{m + m_n}, \quad (\text{A14})$$

and the velocity of the ion in the c.m. frame is

$$\mathbf{v}_{ic} = \frac{m_n}{m + m_n} (\mathbf{v}_i - \mathbf{v}_n). \quad (\text{A15})$$

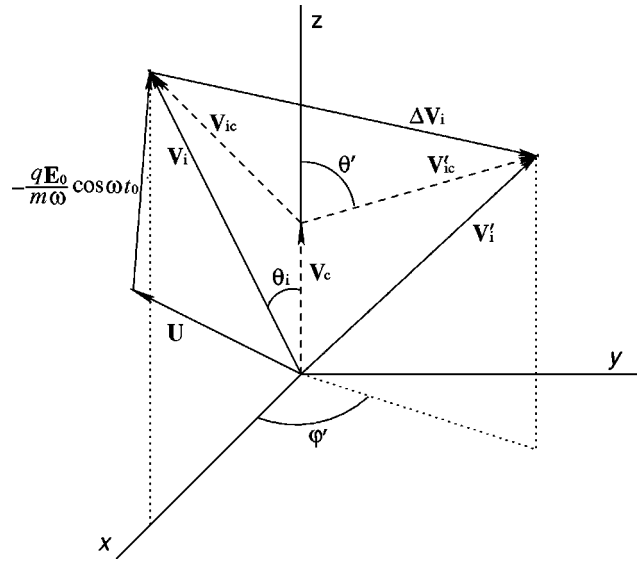


FIG. 6. A vector diagram for the related velocities. While the choosing of the coordinate axis is arbitrary, we choose the direction of \mathbf{v}_c parallel to \hat{z} just for simplicity. \mathbf{v}_n is not shown in this diagram.

Assume the collision is totally elastic between rigid spherical balls. The ion velocity after the collision in the c.m. frame becomes

$$\mathbf{v}'_{ic} = \frac{m_n}{m + m_n} |\mathbf{v}_i - \mathbf{v}_n| \mathbf{i}_{\theta' \varphi'} , \quad (\text{A16})$$

where $\mathbf{i}_{\theta', \varphi'}$ is a unit vector with the spherical coordinates (θ', φ') . Since the collision is between two rigid spherical balls, the spatial distribution of $\mathbf{i}_{\theta', \varphi'}$ is in spherical symmetry. The difference between Eqs. (A15) and (A16) gives the velocity change of the ion after collision,

$$\Delta \mathbf{v}_i = \frac{m_n}{m + m_n} [|\mathbf{v}_i - \mathbf{v}_n| \mathbf{i}_{\theta' \varphi'} + (\mathbf{v}_n - \mathbf{v}_i)]. \quad (\text{A17})$$

Figure 6 is a vector diagram that shows the ion's velocities before and after the collision.

To evaluate the kinetic energy change due to the collision given in Eq. (A12), $|\Delta \mathbf{v}_i|^2$ and $\Delta \mathbf{v}_i \cdot \mathbf{u}$ need to be evaluated. The first term is

$$|\Delta \mathbf{v}_i|^2 = 2 \left(\frac{m_n}{m + m_n} \right)^2 [|\mathbf{v}_i - \mathbf{v}_n|^2 - |\mathbf{v}_i - \mathbf{v}_n|(\mathbf{v}_i - \mathbf{v}_n) \cdot \mathbf{i}_{\theta' \varphi'}]. \quad (\text{A18})$$

The spatial average value for $|\Delta \mathbf{v}_i|^2$ is

$$\langle |\Delta \mathbf{v}_i|^2 \rangle = 2 \left(\frac{m_n}{m + m_n} \right)^2 (v_i^2 + v_n^2), \quad (\text{A19})$$

where we have used

$$\langle |\mathbf{v}_i - \mathbf{v}_n|^2 \rangle = v_i^2 + v_n^2, \quad (\text{A20})$$

which is obtained by averaging over the spherical orientation of \mathbf{v}_n relative to \mathbf{v}_i , and

$$\langle (\mathbf{v}_i - \mathbf{v}_n) \cdot \mathbf{i}_{\theta', \varphi'} \rangle = 0, \quad (\text{A21})$$

which is obtained by averaging over θ' and φ' .

The second term in Eq. (A12) is

$$\Delta \mathbf{v}_i \cdot \mathbf{u} = \left(\frac{m_n}{m + m_n} \right) [|\mathbf{v}_i - \mathbf{v}_n| \mathbf{i}_{\theta', \varphi'} \cdot \mathbf{u} + (\mathbf{v}_n - \mathbf{v}_i) \cdot \mathbf{u}]. \quad (\text{A22})$$

Similarly, by spatial averaging, we obtain

$$\langle \Delta \mathbf{v}_i \cdot \mathbf{u} \rangle = - \left(\frac{m_n}{m + m_n} \right) \left(- \frac{q \mathbf{E}_0}{m \omega} \cos \omega t_0 \cdot \mathbf{u} + u^2 \right). \quad (\text{A23})$$

Substituting Eqs. (A19) and (A23) into Eq. (A12), we have

$$\begin{aligned} \Delta \bar{K} = & \left(\frac{m m_n}{m + m_n} \right) \left\{ \left(\frac{m_n}{m + m_n} \right) \left[\left(- \frac{q \mathbf{E}_0}{m \omega} \cos \omega t_0 + \mathbf{u} \right)^2 + v_n^2 \right] \right. \\ & \left. + \frac{q \mathbf{E}_0}{m \omega} \cos \omega t_0 \cdot \mathbf{u} - u^2 \right\}. \end{aligned} \quad (\text{A24})$$

Since the collision is random over an rf period, the average energy change of the ion due to the collision is

$$\langle \Delta \bar{K} \rangle = \frac{2 m_n^2}{(m + m_n)^2} \frac{q^2 E_0^2}{4 m \omega^2} - \frac{2 m m_n}{(m + m_n)^2} \left(\frac{1}{2} m u^2 - \frac{1}{2} m_n v_n^2 \right) \quad (\text{A25})$$

$$= \frac{2 m_n^2}{(m + m_n)^2} q \psi - \frac{2 m m_n}{(m + m_n)^2} (K_s - K_n), \quad (\text{A26})$$

where $K_n = \frac{1}{2} m_n v_n^2$ is the initial kinetic energy of the atom/molecule. Obviously, the first term represents the rf heating, and, if $K_s > K_n$, the second term represents the collisional cooling.

The time average energy change over the period of the secular motion, using Eqs. (A8) and (A9), is

$$\overline{\langle \Delta \bar{K} \rangle} = \frac{m_n (m_n - m)}{(m + m_n)^2} \bar{W} + \frac{2 m m_n}{(m + m_n)^2} \bar{W}_{\text{neutral}}, \quad (\text{A27})$$

where \bar{W}_{neutral} is the average of K_n . In the case where the temperature of the neutral atom/molecule is much lower than that of the ion in the trap

$$\overline{\langle \Delta \bar{K} \rangle} = \frac{m_n (m_n - m)}{(m + m_n)^2} \bar{W}. \quad (\text{A28})$$

This result shows that the ion will gain energy when the atom/molecule is heavier than the ion, and the ion will lose energy if the atom/molecule is lighter than the ion.

In the case where $m_n < m$, and the rf heating is balanced by the collisional cooling, i.e., $\langle \Delta \bar{K} \rangle = 0$ in Eq. (A27), the final equilibrium ion energy is

$$\bar{W}_f = \frac{2m}{m - m_n} \bar{W}_{\text{neutral}}. \quad (\text{A29})$$

In the extreme case that $m_n \ll m$, the final ion energy is

$$\bar{W}_f = 2 \bar{W}_{\text{neutral}}. \quad (\text{A30})$$

-
- [1] V.G. Anicich and W.T. Huntress, Jr., *Astrophys. J., Suppl.* **62**, 553 (1986).
 [2] R.M. Haberli, T.I. Gombosi, D.L. De Zeeuw, M.R. Combi, and K.G. Powell, *Science* **276**, 939 (1997).
 [3] S. Lepp, A. Dalgarno, and R. McCray, *Astrophys. J.* **358**, 262 (1990).
 [4] W. Liu, A. Dalgarno, and S. Lepp, *Astrophys. J.* **396**, 679 (1992).
 [5] V.H.S. Kwong, D. Chen, and Z. Fang, *Astrophys. J.* **536**, 954 (2000).
 [6] W. Lindinger, D.L. Albritton, and F.C. Fehsenfeld, *J. Chem. Phys.* **62**, 4957 (1975).
 [7] D.A. Church, *Phys. Rep.* **228**, 253 (1993).

- [8] V.H.S. Kwong and Z. Fang, *Phys. Rev. Lett.* **71**, 4127 (1993).
 [9] V.H.S. Kwong, T.T. Gibbons, Z. Fang, J. Jiang, H. Knocke, Y. Jiang, B. Rugar, S. Huang, E. Braganza, and W. Clark, *Rev. Sci. Instrum.* **61**, 1931 (1990).
 [10] R.D. Knight and M.H. Prior, *J. Appl. Phys.* **50**, 3044 (1979).
 [11] F.A. Parpia and W.R. Johnson, *Phys. Rev. A* **26**, 1142 (1982).
 [12] Z. Fang and V.H.S. Kwong, *Astrophys. J.* **474**, 529 (1997).
 [13] A.V. Gaponov and M.A. Miller, *J. Exp. Theor. Phys.* **34**, 242 (1958).
 [14] H.G. Dehmelt, in *Advances in Atomic and Molecular Physics*, edited by D.R. Bates and I. Estermann (Academic, New York, 1967), Vol. 3, p. 53.